

Two-center basis generator method calculations for Li^{3+} , C^{3+} and O^{3+} ion impact on ground state hydrogen

Anthony C. K. Leung and Tom Kirchner*

*Department of Physics and Astronomy,
York University, Toronto, Ontario, M3J 1P3, Canada*

(Dated: January 25, 2022)

arXiv:2112.12863v2 [physics.atom-ph] 21 Jan 2022

Abstract

The two-center basis generator method is used to obtain cross sections for excitation, capture, and ionization in Li^{3+} , C^{3+} , and O^{3+} collisions with ground-state hydrogen at projectile energies from 1 to 100 keV/u. The interaction of the C^{3+} and O^{3+} projectiles with the active electron is represented by a model potential. Comparisons of cross sections with previously reported data show an overall good agreement, while discrepancies in capture for C^{3+} collisions at low energies are noted. The present results show that excitation and ionization are similar across the three collision systems, which indicates that these cross sections are mostly dependent on the net charge of the projectile only. The situation is different for the capture channel.

I. INTRODUCTION

Collisions between partially stripped ions and neutrals (atoms or molecules) are more commonly found in nature than collisions with bare ions. Partially stripped ion collisions have been a subject of interest in astrophysical [1, 2] and plasma applications [3], and thus, interest in accurate cross sections for electronic processes in these collisions remains high. In recent times, the International Nuclear Data Committee within the International Atomic Energy Agency has expressed interest in cross sections from collisions between bare or partially stripped projectiles with atomic hydrogen, which are necessary for neutral beam modeling in fusion plasma [4].

In this study, new calculated cross sections for collision systems involving ground-state hydrogen and ions of net charge $Q = 3$ are reported. Specifically, the projectile ions Li^{3+} , C^{3+} and O^{3+} were chosen for this analysis. Cross sections for electron excitation, capture, and ionization are compared with the data that are available in the literature. Currently, there is a broad coverage of cross sections for Li^{3+} -H(1s) collisions from the low- to the high-energy regimes (e.g., References [5–7]). Although data exist for C^{3+} and O^{3+} collisions with atomic hydrogen [8–10], there are some gaps for excitation and ionization data in the intermediate energy regime. Therefore, the objectives of this study are to report cross sections in these gaps, perform validity checks on existing ones, and provide a comparison for the three ions to determine to what extent the net charge alone determines the cross sections.

The approach used in the present theoretical analysis is the semiclassical, nonperturbative

* tomk@yorku.ca

two-center basis generator method (TC-BGM) [11]. As a close-coupling approach, the main feature of the TC-BGM is its dynamical basis that is adapted to the problem at hand, which provides a practical advantage in terms of reaching convergence with smaller basis sets than required in standard approaches. It is relevant to this study that the TC-BGM was previously used in References [12, 13] to obtain accurate capture and ionization cross sections for $\text{Li}^{3+}\text{-H}(1s)$ collisions at impact energies of 10 keV/u and higher. The present work focuses on collisions at impact energies from 1 to 100 keV/u.

The article is organized as follows: In Section II, an overview of the TC-BGM for ion–atom collisions is given. In Section III, cross sections for the three collision systems are presented and discussed. Finally, in Section IV, concluding remarks are provided. Atomic units ($\hbar = e = m_e = 4\pi\epsilon_0 = 1$) are used throughout the article unless stated otherwise.

II. THEORETICAL METHOD

The focus of this study is on collisions in the low- and intermediate-impact energy regimes, specifically from 1 to 100 keV/u. The collisional framework used here is based on the impact-parameter model within the semiclassical approximation. Such a framework has been used with the TC-BGM to solve the time-dependent Schrödinger equation (TDSE) in previous studies and has also been described at some length in a prior work related to collisions with atomic hydrogen [14]. For this reason, only a summary highlighting the core ideas and some details regarding the potentials used are given.

In the laboratory frame, the hydrogen target is assumed to be fixed in space and the projectile ion travels in a straight-line path at constant speed v_P , described by $\mathbf{R}(t) = (b, 0, v_P t)$, where b is the impact parameter. The objective is to solve the TDSE for the initially occupied ground state in the target,

$$i\frac{\partial}{\partial t}\psi(\mathbf{r}, t) = \hat{h}(t)\psi(\mathbf{r}, t). \quad (1)$$

For the present study, the projectile ions under consideration are Li^{3+} , C^{3+} , and O^{3+} . This study assumes that the strongly bound electrons in the C^{3+} and O^{3+} ions remain frozen during the collision. This allows the single-particle Hamiltonian to be decomposed as

$$\hat{h}(t) = -\frac{1}{2}\nabla^2 + V_T(|\mathbf{r}|) + V_P(|\mathbf{r}_P|, t), \quad (2)$$

where \mathbf{r}_P is the electron position vector with respect to the projectile and is related to that with

respect to the target by $\mathbf{r}_P(t) = \mathbf{r} - \mathbf{R}(t)$. The projectile Li^{3+} is represented by the Coulomb potential with $Z_P = 3$. For the C^{3+} projectile, two sets of cross sections are produced, where one is generated using the optimized potential model (OPM) [15] and another one using the two-parameter analytic potential model of Green, Sellin, and Zachor (GSZ) [16]. The potential for the O^{3+} projectile is represented with the GSZ model.

The GSZ model can be viewed as a modified Hartree–Fock procedure in which the expectation value of the many-electron Hamiltonian is minimized with respect to a determinantal wave function constructed from orbitals which satisfy a one-electron Schrödinger equation with the GSZ potential. The minimization fixes the two parameters involved. For the calculations of this work, we use the parameters reported in Ref. [17] for the $\text{C}^{2+}(1s^2 2s^2)$ and the $\text{O}^{2+}(1s^2 2s^2 2p^2)$ configurations such that the GSZ potentials exhibit the correct asymptotic behavior from the viewpoint of an additional electron. One can criticize this procedure for erroneously assuming that electron transfer to the projectile produces a doubly charged ground-state ion, while in reality electron capture mostly populates excited projectile states (except at very high impact energies). However, it turns out that the orbital energy eigenvalues obtained from solving the one-electron Schrödinger equation with the GSZ potential are reasonably close to experimentally determined spectroscopic data [18]. In the case of carbon, for example, they do not deviate more than 5% for the $n = 3$ shell, which is the dominant capture shell for most of the impact energy range studied here. In addition, no assumption on the configuration in the projectile after electron capture is made when generating the OPM potential and the corresponding bound states, which we use as an alternative. In this case, we start with a fully numerical self-consistent potential for the $\text{C}^{3+}(1s^2 2s)$ ion and subtract the exchange part in order to represent the situation for an additional electron which does not contribute to the charge distribution on the projectile. This procedure is explained in Ref. [19]. The results obtained from both variants indicate that relatively small changes in the potential model do not cause major discrepancies in the cross sections (see Sec. III B).

The TDSE (1) is solved by projection onto a finite set of basis states and propagation using the TC-BGM. The basis sets that were used for this analysis include: all nlm states from $n = 1$ to $n = 5$ of the hydrogen target, states from $n = 1$ to $n = 6$ of Li^{2+} , states from $n = 2$ to $n = 6$ of C^{2+} and O^{2+} ions, and 45 BGM pseudostates to account for intermediate quasimolecular couplings and ionization to the continuum. Details on the construction of the pseudostates and the calculation of matrix elements can be found in Ref. [20]. Bound-state probabilities for

finding the electron on the target p^{tar} or on the projectile p^{cap} are calculated from summing up the transition probabilities within the bound-state basis sets, and probabilities for total ionization p^{ion} are obtained from the unitarity criterion

$$p^{\text{ion}} = 1 - p^{\text{tar}} - p^{\text{cap}}. \quad (3)$$

Finally, cross sections for the electronic transitions are obtained by integrating the probabilities over the impact parameter

$$\sigma = 2\pi \int_0^{b_{\text{max}}} bp(b)db, \quad (4)$$

where b_{max} (in a.u.) is the upper bound at which the integral is cut in practice. For the collision calculations reported here, an upper bound of $b_{\text{max}} = 20$ a.u. was more than sufficient to capture the asymptotic profile of these transition probabilities. It should also be noted that the conservation of unitarity (3) was monitored in the present analysis by summing up the transition probabilities to all BGM pseudostates after orthogonalizing them to the bound-state basis sets. It was found that deviations produced by the calculations are typically no larger than 1%.

III. RESULTS AND DISCUSSION

A. $\text{Li}^{3+}\text{-H}(1s)$

The cross section results for the $\text{Li}^{3+}\text{-H}(1s)$ collision system are shown in Figure 1. Starting with the n -state excitation cross sections (Figure 1a), the present TC-BGM results are compared with other calculations. The work by Suarez *et al.* [21] reported recommended excitation cross sections based on the two-center one-electron diatomic molecule expansion covering 1 to 80 keV/u and the one-center Bessel expansion that covers energies greater than 80 keV/u. The work by Agueny *et al.* [22] was based on the two-center atomic orbital close-coupling method with Gaussian-type orbitals (TC-AOCC-GTO). Only the excitation of the $n = 2$ and $n = 3$ shells are presented, since transitions to higher energy states are not important at these impact energies [21]. It is shown that the present TC-BGM results are in satisfactory agreement with previously reported cross sections [21, 22].

In Figure 1b, total electron capture cross sections for the $\text{Li}^{3+}\text{-H}(1s)$ collision system are shown. The present TC-BGM capture results show an impact-energy dependence, which is

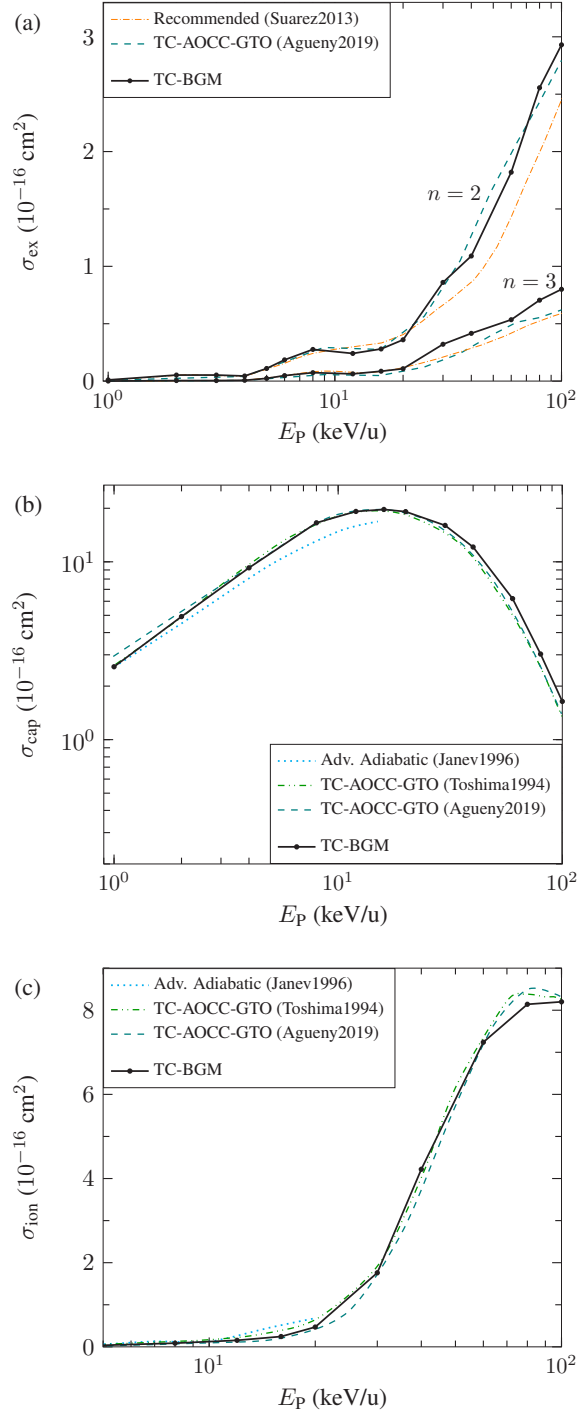


FIG. 1. Cross sections of (a) target-excitation, (b) electron capture, and (c) ionization for $\text{Li}^{3+}\text{-H}(1s)$ collisions from 1 to 100 keV/u. Recommended data from Ref. [21]. Theory: present TC-BGM, TC-AOCC-GTO [22, 23], and Advanced Adiabatic [24].

consistent with previously reported results, namely, the TC-AOCC-GTO [22], another TC-AOCC-GTO calculation by Toshima [23], and the advanced adiabatic method by Janev *et al.* [24]. Quantitatively, the present cross sections are closest to the TC-AOCC-GTO results [22, 23] at all impact energies. There are some differences in the advanced adiabatic calculations [24] compared with the present results but they are no more than 20%, and smaller at low energies where the advanced adiabatic method [24] is expected to work best.

Figure 1c shows the ionization results for $\text{Li}^{3+}\text{-H}(1s)$ collisions. The present cross sections are compared with those from the advanced adiabatic [24] and TC-AOCC-GTO [22, 23] calculations. It can be seen that the present TC-BGM results are consistent with the previous calculations and show that ionization is important in the intermediate energy regime at 10 keV/u and above but negligible at lower energies. They are also consistent with the aforementioned studies [12, 13] using the TC-BGM on $\text{Li}^{3+}\text{-H}(1s)$ collisions at 10 keV/u and above. Overall, the cross sections produced by the TC-BGM are in good agreement with previous calculations.

B. $\text{C}^{3+}\text{-H}(1s)$

Shown in Fig. 2 are the cross section results for C^{3+} collisions with ground-state hydrogen. The n -state excitation cross sections in Fig. 2a only include results from the present TC-BGM calculations since, to our knowledge, no other results are available in the literature. Two sets of results from TC-BGM calculations are shown, where one set is based on using the OPM to represent the partially stripped ion and the other set is based on the GSZ potential. The excitation cross sections show the typical increasing behavior as the impact energy increases. There are some discrepancies between the OPM and GSZ results around 100 keV/u but these differences decrease towards lower energies. Similar to Li^{3+} collisions, the dominant excitation channel in the $\text{C}^{3+}\text{-H}(1s)$ system is $n = 2$ followed by $n = 3$. One can also see the qualitative and quantitative similarities in the cross section profiles of these two systems with excitation processes being important at 20 keV/u and higher. This observation reflects the fact that the target electron mainly experiences an overall net charge of $Q = 3$ (i.e., the same as for Li^{3+} impact) and that non-Coulombic interactions are of minor importance.

In Fig. 2b, the total capture cross sections for $\text{C}^{3+}\text{-H}(1s)$ collisions are presented. Again, two sets of TC-BGM results are shown where one set is based on using the OPM for the projectile while the other one is based on the GSZ potential. Shown alongside the present

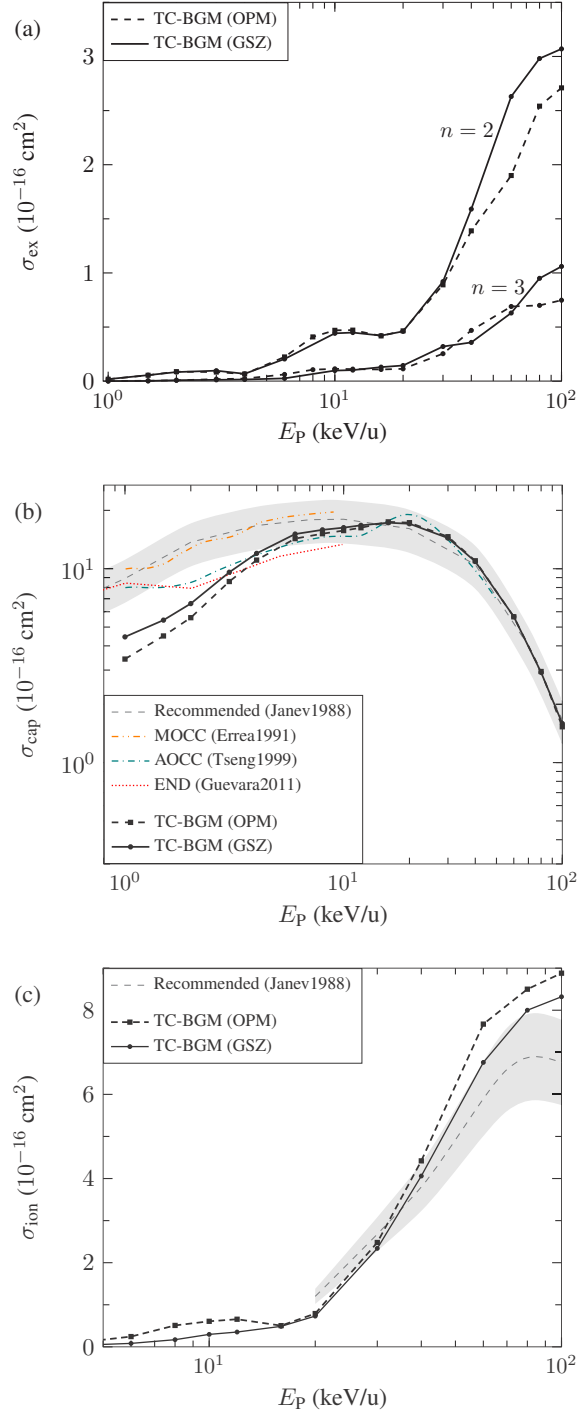


FIG. 2. Cross sections for C^{3+} -H(1s) collisions from 1 to 100 keV/u: (a) target-excitation; (b) electron capture; (c) ionization. Recommended data from Ref. [8]. Theory: present TC-BGM, MOCC [9], AOCC [25], and END [10].

cross sections are previously reported values from calculations using a molecular-orbital close-coupling (MOCC) scheme [9], calculations using an AOCC expansion [25], calculations based on the electron nuclear dynamics (END) approach [10], and a set of recommended values based on theoretical and experimental works compiled by Janev *et al.* [8] with a 25% uncertainty band. Both the MOCC calculation [9] and the AOCC calculation [8] are explicit two-electron calculations. One can see that the TC-BGM cross sections at low energies are significantly lower than the previously reported results. Between the two sets of the present TC-BGM results, the capture cross section produced from using the GSZ potential is slightly closer to previous results than those that obtained from using the OPM. The discrepancies at low energies could be due to the present treatment of the C^{3+} projectile, which assumes that the screening of the nucleus is frozen throughout the course of the collision. Interestingly, the differences in capture between the OPM and GSZ results decrease as impact energy increases; the opposite tendency is seen for excitation (Fig. 2a).

The overall agreement of the present TC-BGM ionization cross sections with the recommended values [8] shown in Fig. 2c is satisfactory. The cross section profile from the present calculations shows the expected behavior where ionization is not important at 10 keV/u and below. At higher energies, one can see the typical profile of an increasing cross section. One can also see the quantitative similarities of Li^{3+} and C^{3+} impact between 10 and 100 keV/u. Overall, it appears that the present cross section calculated using the GSZ potential is closer to the recommended values than the results that are based on the OPM.

Figure 3 illustrates the differences between the OPM and the GSZ potentials, where the r -weighted potentials are plotted with respect to the radial distance. The potential profiles show identical asymptotic behaviors at short and long distances but display some differences in the $r \in [0.01, 1]$ a.u. interval where the GSZ potential is mostly lower than the OPM. In other words, the GSZ models a potential that is more attractive than the OPM.

C. O^{3+} -H(1s)

Figure 4 shows the set of cross sections for O^{3+} -H(1s) collisions. The excitation cross sections in Fig. 4a show the typical increasing behavior between 1 and 100 keV/u. Moreover, one can again see that the dominant channel is $n = 2$ and the quantitative similarities to the results for Li^{3+} and C^{3+} collisions. Specifically, a cross section value of approximately 3×10^{-16} cm² for

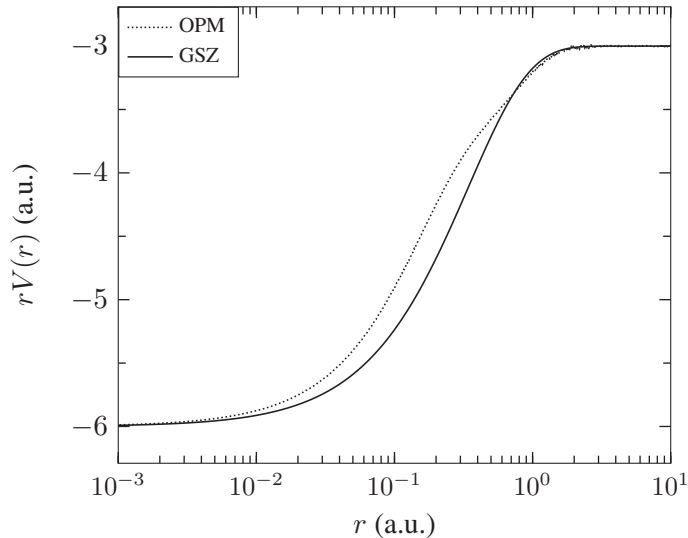


FIG. 3. Distance-weighted effective potential of the C^{3+} projectile as a function of radial distance. Potentials calculated using the OPM [15] and GSZ [17] are displayed.

the $n = 2$ channel is obtained at 100 keV/u across all three collision systems.

In Fig. 4b, the total capture cross sections calculated from the present TC-BGM are compared with the previously reported recommended values [8] and the more recent results from END calculations [10]. The present results are quantitatively consistent with the previous results and are within the uncertainty range of the recommended values [8]. This is in contrast to the observation that was made for the capture cross section in C^{3+} collisions (Fig. 2b), where discrepancies with the END and with other calculations are significant at low impact energies. In addition, the capture profile here is noticeably different from that of the Li^{3+} (Fig. 1b) and C^{3+} (Fig. 2b) collisions, with capture by O^{3+} ions showing a monotonic decrease over the entire energy range displayed.

Figure 4c shows the total ionization cross section. The present TC-BGM results are compared with the previously compiled recommended values [8]. One can see that the present results are well within the uncertainty range of the recommended values between 40 and 100 keV/u but fall short at lower energies. Given that only these recommended values are available, additional independent studies are necessary to provide further validation of the present results.

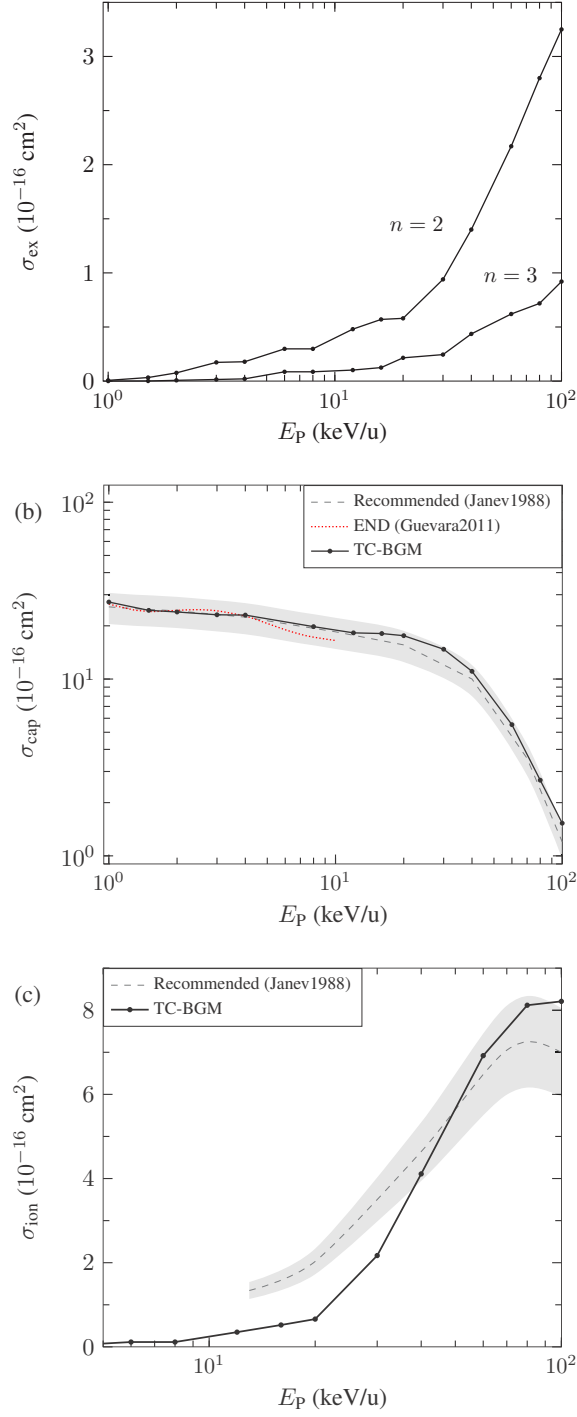


FIG. 4. Cross sections for O^{3+} -H collisions from 1 to 100 keV/u: (a) target-excitation; (b) electron capture; (c) ionization. Recommended data from Ref. [8]. Theory: present TC-BGM and END [10].

IV. CONCLUSIONS

In this work, we reported TC-BGM cross section calculations for Li^{3+} , C^{3+} , and O^{3+} collisions with ground-state hydrogen from 1 to 100 keV/u. Cross sections for electron excitation, capture, and ionization were obtained for all three systems. Overall, we found satisfactory agreement between the present cross sections and previously reported values.

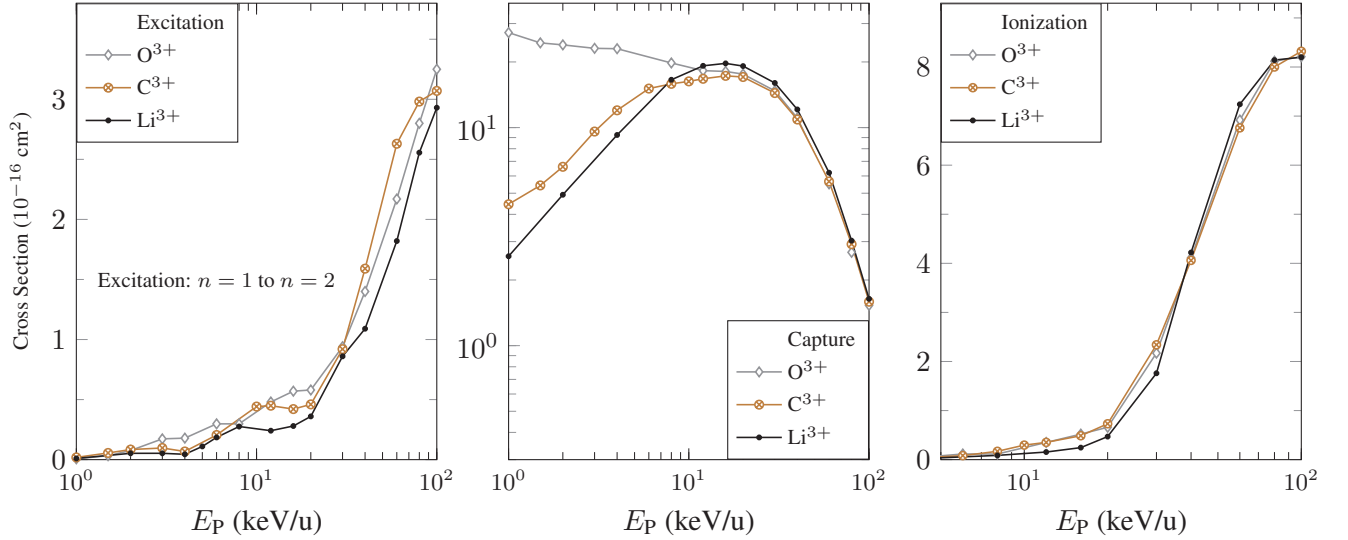


FIG. 5. TC-BGM cross sections of Li^{3+} -, C^{3+} -, and O^{3+} - $\text{H}(1s)$ collisions plotted with respect to impact energies for target-excitation from $n = 1$ to $n = 2$ (left panel), total electron capture (middle panel), and total ionization (right panel).

We also drew a few comparisons of the cross sections across the different projectiles. This is summarized in Fig. 5 where total cross sections for excitation, capture, and ionization for all three collision systems are plotted together. One can observe the similarities in the energy dependence of the excitation and ionization cross sections across the three systems. For capture, differences in cross sections are significant at 10 keV/u and below, indicating that the precise form of the screening of the projectile nucleus matters.

ACKNOWLEDGMENTS

Financial support from the Natural Sciences and Engineering Research Council of Canada (NSERC) (RGPIN-2019-06305) is gratefully acknowledged. This work was made possible with the high-performance computing resources provided by Compute/Calcul Canada.

APPENDIX

The cross section data from the TC-BGM calculations for Li^{3+} , C^{3+} , and O^{3+} collisions with ground-state hydrogen are presented in Tables I, II, and III. For the C^{3+} and O^{3+} projectiles the GSZ potential has been used.

TABLE I. n -state selective excitation cross sections (10^{-16} cm^2) for Li^{3+} , C^{3+} , and O^{3+} collisions with ground-state hydrogen from 1 to 100 keV/u.

E(keV/u)	$\text{Li}^{3+}\text{-H}(1s)$		$\text{C}^{3+}\text{-H}(1s)$		$\text{O}^{3+}\text{-H}(1s)$	
	n=2	n=3	n=2	n=3	n=2	n=3
1	0.010	0.001	0.019	0.001	0.007	<0.001
2	0.053	0.005	0.084	0.009	0.076	0.007
3	0.053	0.005	0.097	0.012	0.173	0.015
4	0.045	0.007	0.068	0.016	0.179	0.021
6	0.185	0.048	0.205	0.026	0.298	0.086
8	0.276	0.074	0.442	0.098	0.341	0.071
12	0.241	0.063	0.449	0.102	0.480	0.102
16	0.280	0.086	0.421	0.130	0.570	0.125
20	0.360	0.108	0.460	0.145	0.580	0.215
30	0.860	0.321	0.920	0.320	0.940	0.245
40	1.090	0.416	1.590	0.358	1.400	0.436
60	1.820	0.535	2.630	0.630	2.170	0.620
80	2.556	0.705	2.981	0.950	2.800	0.718
100	2.930	0.800	3.070	1.060	3.250	0.920

TABLE II. Total-capture cross sections (10^{-16} cm²) for Li³⁺, C³⁺, and O³⁺ collisions with ground-state hydrogen from 1 to 100 keV/u.

E(keV/u)	Li ³⁺ -H(1s)	C ³⁺ -H(1s)	O ³⁺ -H(1s)
1	2.57	4.45	27.26
2	4.92	6.61	23.95
3	7.24	9.59	23.09
4	9.25	12.00	23.00
6	13.86	15.10	21.10
8	16.57	15.87	19.79
12	19.20	16.74	18.25
16	19.70	17.27	18.09
20	19.15	17.06	17.59
30	16.02	14.40	14.74
40	12.11	10.89	11.06
60	6.21	5.66	5.52
80	3.03	2.92	2.68
100	1.64	1.59	1.53

TABLE III. Total-ionization cross sections (10^{-16} cm^2) for Li^{3+} , C^{3+} , and O^{3+} collisions with ground-state hydrogen from 1 to 100 keV/u.

E(keV/u)	$\text{Li}^{3+}\text{-H}(1s)$	$\text{C}^{3+}\text{-H}(1s)$	$\text{O}^{3+}\text{-H}(1s)$
1	< 0.001	0.002	0.001
2	0.003	0.011	0.007
3	0.006	0.026	0.030
4	0.014	0.028	0.034
6	0.042	0.082	0.115
8	0.087	0.172	0.115
12	0.155	0.352	0.350
16	0.245	0.487	0.502
20	0.466	0.731	0.660
30	1.760	2.340	2.173
40	4.215	4.056	4.019
60	7.236	6.757	6.811
80	8.141	8.003	8.118
100	8.198	8.320	8.209

-
- [1] T. E. Cravens, *Astrophys. J.* **532**, L153 (2000).
- [2] O. Abu-Haija, J. A. Wardwell, and E. Y. Kamber, *J. Phys. Conf. Ser.* **58**, 195 (2007).
- [3] H. Bruhns, H. Kreckel, D. W. Savin, D. G. Seely, and C. C. Havener, *Phys. Rev. A* **77**, 064702 (2008).
- [4] H.-K. Chung, *Data for Atomic Processes of Neutral Beams in Fusion Plasma Summary Report of the First Re*
Tech. Rep. (International Atomic Energy Agency (IAEA), 2017).
- [5] M. B. Shah, T. V. Goffe, and H. B. Gilbody, *J. Phys. B* **11**, 2 (1978).
- [6] W. Fritsch and C. D. Lin, *J. Phys. B* **15**, L281 (1982).
- [7] I. Murakami, J. Yan, H. Sato, M. Kimura, R. K. Janev, and T. Kato, *At. Data Nucl. Data Tables* **94**, 161 (2008).
- [8] R. Janev, R. Phaneuf, and H. Hunter, *At. Data Nucl. Data Tables* **40**, 249 (1988).
- [9] L. F. Errea, B. Herrero, L. Méndez, O. M6, and A. Riera, *J. Phys. B* **24**, 4049 (1991).
- [10] N. L. Guevara, E. Teixeira, B. Hall, Y. Öhrn, E. Deumens, and J. R. Sabin, *Phys. Rev. A* **83**, 052709 (2011).
- [11] M. Zapukhlyak, T. Kirchner, H. J. Lüdde, S. Knoop, R. Morgenstern, and R. Hoekstra, *J. Phys. B* **38**, 2353 (2005).
- [12] H. J. Lüdde, T. Kalkbrenner, M. Horbatsch, and T. Kirchner, *Phys. Rev. A* **101**, 062709 (2020).
- [13] H. J. Lüdde, A. Jorge, M. Horbatsch, and T. Kirchner, *Atoms* **8**, 10.3390/ATOMS8030059 (2020).
- [14] A. C. K. Leung and T. Kirchner, *Eur. Phys. J. D* **73**, 246 (2019).
- [15] E. Engel and S. H. Vosko, *Phys. Rev. A* **47**, 2800 (1993).
- [16] A. E. S. Green, D. L. Sellin, and A. S. Zachor, *Phys. Rev.* **184**, 1 (1969).
- [17] P. P. Szydlík and A. E. Green, *Phys. Rev. A* **9**, 1885 (1974).
- [18] A. Kramida, Y. Raichenko, J. Reader, and N. A. T. (2021),
NIST Atomic Spectra Database (version 5.9) (2021).
- [19] G. Schenk and T. Kirchner, *Phys. Rev. A* **91**, 052712 (2015).
- [20] H. J. Lüdde, M. Horbatsch, and T. Kirchner, *Eur. Phys. J. B* **91**, 10.1140/epjb/e2018-90165-x
(2018).
- [21] J. Suarez, F. Guzman, B. Pons, and L. F. Errea, *J. Phys. B* **46**, 10.1088/0953-4075/46/9/095701
(2013).

- [22] H. Agueny, J. P. Hansen, A. Dubois, A. Makhoute, A. Taoutioui, and N. Sisourat, [At. Data Nucl. Data Tables **129-130**, 101281 \(2019\)](#).
- [23] N. Toshima, [Phys. Rev. A **50**, 3940 \(1994\)](#).
- [24] R. K. Janev, E. A. Solov'ev, and Y. Wang, [J. Phys. B **29**, 2497 \(1996\)](#).
- [25] H. C. Tseng and C. D. Lin, [J. Phys. B **32**, 5271 \(1999\)](#).